JOURNAL OF SPACECRAFT AND ROCKETS
Vol. 30, No. 1, January-February 1993

Analysis and Sizing of Mars Aerobrake Structure

I. S. Raju*
Analytical Services & Materials, Inc., Hampton, Virginia 23666
and
W. J. Craft†
North Carolina A&T State University, Greensboro, North Carolina 27411

A cone-sphere aeroshell structure for aerobraking into Martian atmosphere is studied. Using this structural configuration, a space frame load-bearing structure is proposed. To generate this structure efficiently and to perform a variety of studies of several configurations, a mesh generator that utilizes only a few configurational parameters is developed. A finite element analysis program that analyzes space frame structures was developed. A sizing algorithm that arrives at a minimum mass configuration was developed and integrated into the finite element analysis program. A typical 135-ft-diam aerobrake configuration was analyzed and sized. The minimum mass obtained in this study using high modulus graphite/epoxy composite material members is compared with the masses obtained from two other aerobrake structures using lightweight erectable tetrahedral truss and part-spherical truss configurations. Excellent agreement for the minimum mass was obtained with the three different aerobrake structures. Also, the minimum mass using the present structure was obtained when the supports were not at the base but at about 75% of the base diameter.

Nomenclature

A	= area of cross section of the space frame member, in.^{2}
D	= diameter at the base of the aerobrake structure (see Fig. 1), in.
E, G	= Young's modulus and shear modulus of the material, psi
$F_{x'}$, $F_{y'}$, $F_{z'}$	= forces at either end of a space frame member in the local member coordinate, (x', y', z') system, lbf
$I_{y'y'}$, $I_{z'z'}$	= moments of inertia of a space frame member about y' and z' axes, respectively, in.^{4}
l	= length of a space frame member, in.
$M_{x'}$, $M_{y'}$, $M_{z'}$	= moments at either end of a space frame member about the local member coordinate (x', y', z') system, in.-lb
p	= normal aerodynamic pressure on the aeroshell, psi
R_o	= outer radius of a tubular space frame member, in.
R_{o_n}	= new outer radius of a space frame member computed by the sizing algorithm, in.
t	= thickness of a tubular space frame member (strut), in.
$t_{\min}$	= minimum thickness of strut material stock, in.
t_n	= new thickness of struts computed by the sizing algorithm, in.
W_j	= mass of the aerobrake structure at the end of the jth iteration, lbm
$w(x', y')$	= deflection of at any point (x', y') of a quadrilateral panel element on the aeroshell, in.
X, Y, Z	= Cartesian coordinate system (see Fig. 2)
x', y', z'	= local member coordinate or the local quadrilateral panel system (see Fig. 3)
Σ_T, Σ_C	= tension and compression allowables for the strut material, respectively, psi
σ_T, σ_C	= maximum tensile and compressive stresses in the members, respectively, psi

Received March 23, 1992; revision received June 19, 1992; accepted for publication June 22, 1992.

*Senior Scientist. Associate Fellow AIAA.
†Chairman and Professor, Department of Mechanical Engineering.

Introduction

THE purpose of the Mars aerobrake is to decelerate the spacecraft from Earth to Mars to orbital speed around the planet. This is accomplished by the drag imposed by the upper atmosphere on the umbrella-like structure at the forward end of the spacecraft. The aerobrake is a lightweight large composite shell with a supporting beam member substructure designed to transmit deceleration loads to the spacecraft payload. It is important that minimum weight structures be developed for aerobraking maneuvers within the upper atmosphere of the planet Mars if humans and instrumentation packages are to explore that planet during the first and second decades of the 21st century. It is equally important to prove the feasibility of the concept in comparison with existing technologies, including the use of retrorockets and nuclear-powered thrusters that accomplish the same function. Propulsion braking technology is well understood, and an aerobrake must show an undisputable weight advantage while exhibiting a high reliability and safety margin with current structural materials.

The purpose of this paper is to present an analysis and sizing of a cone-sphere-type aerobrake structural configuration. The space-frame-type load-bearing structure is proposed. The structure is assumed to be loaded by the aerodynamic pressure on the aeroshell, and this loading on the aeroshell is assumed to be transmitted through the heat shield and the underlying structure to the space frame structure. A sizing algorithm is presented that considers various possible stress conditions (tension, compression, bending, and buckling loads) of each space frame member. The sizing algorithm arrives at the optimal cross-sectional area of each member, and the algorithm is integrated into the finite element (FE) analysis program. First, the aerobrake configuration and the mesh generator are presented. Next, the details of the loading are given. Third, the analysis and the sizing procedure are explained. Next, the results of the analysis and the sizing for a typical 135-ft aerobrake space frame structure are presented. The minimum mass obtained by the present algorithm is compared with those available in the literature.

Aerobrake Configuration

An aerobrake with a cone-sphere configuration as shown in Fig. 1 is assumed. The cone-sphere configuration was chosen for the study because it represents a class of conics that are capable of producing a variety of lift-to-drag ratios. This configuration shown in Fig. 1 has an L/D ratio of nearly 0.2 and is used in Mars re-entry studies.[1-6] This aerobrake represents a typical aerobrake and is utilized as a vehicle to develop and evaluate the analysis and sizing methods presented in this paper and also to study typical aerobrake masses that are required to withstand the anticipated aerodynamic loading.

In this paper the following assumptions are made.

1) The aerobrake structure is assumed to be a cold structure, i.e., the aerodynamic heating that occurs in the re-entry is assumed to be taken into account by the thermal protection system, and the load-bearing structure does not encounter any thermal loading (or thermal cycling).

2) Inertial loads of the aerobrake structure are neglected. This assumes that the mass of the aerobrake is much smaller than the total load on the structure due to deceleration.

3) The structural configuration carries all of the load. This assumes that the thermal protection system is not a load-bearing structure and that it efficiently transmits the loads to the structure. Also, the payload is assumed to be rigid and not to suffer any deformations due to the loading.

4) In the analysis presented in this paper a constant aerodynamic pressure is assumed and is assumed to act normal to all of the wetted surfaces of the aerobrake. The loading algorithm is built so as to take into consideration any nonuniform pressure distribution. However, the "worst case" scenario is to consider the maximum aerodynamic pressure as a constant pressure on all of the wetted surface. If the aerobrake mass is competitive with the mass due to propulsion braking, then the actual aerobrake mass with varying pressure distribution will also be even more competitive.

5) A factor of safety of 1.4 is used. The loading is scaled up by a factor of 1.4 and is used in the analysis.

Geometric Model

The outer shell of the aerobrake is assumed to be composed of conic sections of a sphere and a cone. Figure 1 shows the particular configuration used in this study. A cone with a 60-deg semivertex angle joined to a sphere of radius 51.9 ft was chosen. The cone-sphere intersects in a circle where both the curves and their slopes match. The base of the cone was 135 ft in diameter and the distance from the base to the forward point was 30.45 ft with a height-to-base ratio of $30.45/135 = 0.23$. An asymmetrical shell can be generated by using a nonzero angle β of the oblique cutting plane. In addition, the forward end of the aerobrake can be left open with a hole by the introduction of an angle ϕ_o. Thus the entire outer shell, Fig. 1, can be generated by five parameters:

- h = distance from the cone's (fictitious) vertex to the base of the cone
- h_{sl} = distance from the center of the sphere to the vertex of the cone
- β = inclination of base cutting plane to axis of cone ($\beta = 0$ for a symmetric cone)
- α = semivertex angle of the cone
- ϕ_o = angle defining the innermost location on the sphere where there is a hole or cutout
- $\phi_o = 0$ = a sphere with no cutout or one completely covering the forward section of the aerobrake, hole diameter = $2h \sin(\alpha) \sin(\phi_o)$

Once the generating parameters are in place, then the outer surface is partitioned into "petals" that sweep equal azimuthal increments about the conical axis (see Figs. 2 and 3). Along each of these arcs from the forwardmost point of the spherical portion to the aft point of the cone at the base, any number of equally spaced points may be erected along the spherical and conical surfaces. The number of increments along a spherical section J_{sp} and the number of increments along the conical section J_c define a series of outer surface nodes along each petal. These, along with the number of increments along the azimuth J_θ, determine the total nodes of

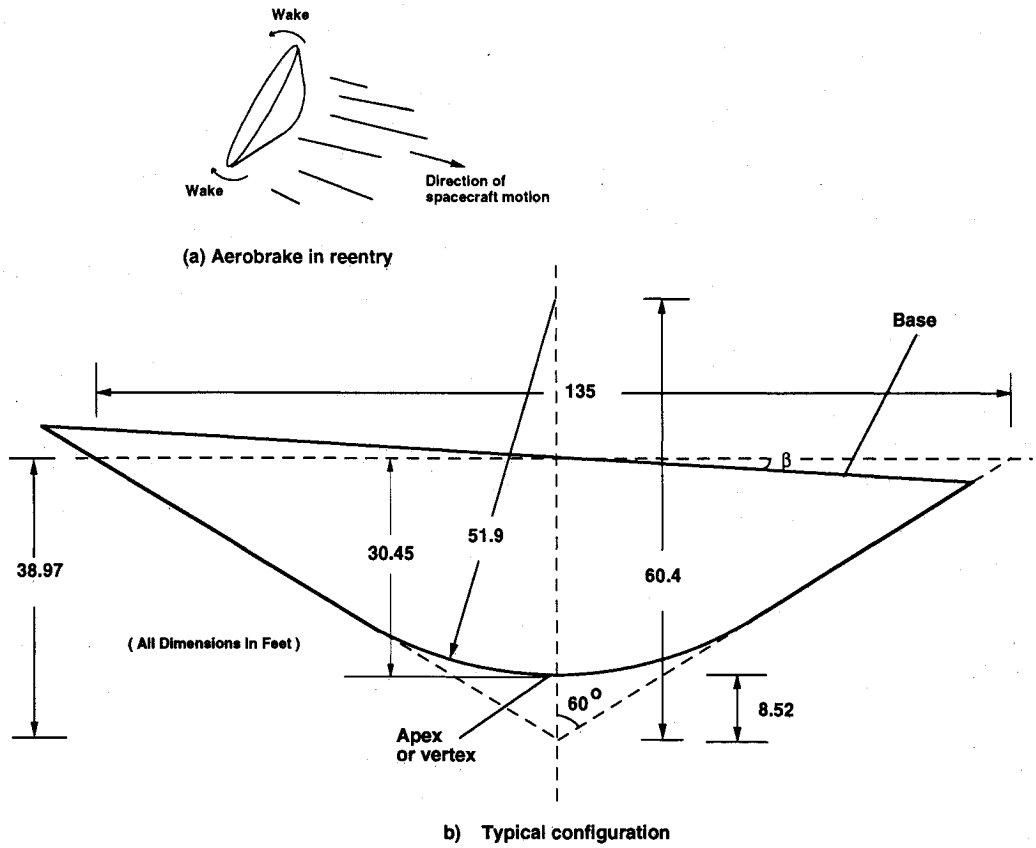

Fig. 1 Typical Mars aerobrake configuration.

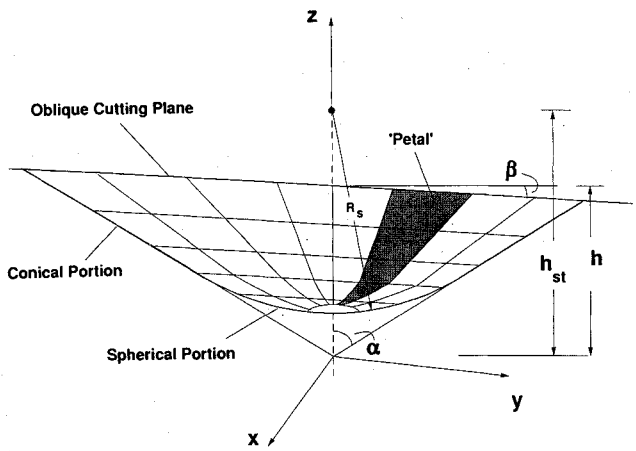

Fig. 2 Parameters used in the mesh generator.

the outer surface. The total number of nodes can be computed from

$$N = (J_{sp} + J_C + 1) \times J_\theta$$

Note that the nodes determine the location of the joints of the space frame. At each of these outer surface nodes, normals to the surface are erected and these normals end at the inner surface nodes. The length of these normals from the outer surface to the inner surface nodes equals the depth or thickness of the aerobrake structure at that location. In the studies that follow, these normals were all assumed to be equal and hence constant depth aerobrakes were analyzed. However, there are provisions for the depth to be a variable and the only restriction is that they remain constant for a given position along a petal while the azimuth is incremented (see Fig. 3).

Adjacent nodes on adjacent petals and their inward normals form a space quadrilateral. Each quadrilateral is connected internally so that a diagonally stable structure results as a space frame and each frame is attached to its neighboring space frame to form the substructure of the aerobrake (see Fig. 3).

Load-Bearing Structure

In this paper the load-bearing structure of the aerobrake is assumed to be built with space frame members (see Fig. 3). The space frame members are capable of reacting the three forces along and three moments about each of the coordinate directions at the joints. Instead, one could also assume that the structure consists only of space truss members with pin joints so that there are no moments. Neither assumption, space frame nor space truss, is realistic, and each represents an extreme condition whereas the reality is somewhere in the middle. Thus, as a first step the space frame assumption is invoked. The load-bearing structure is constructed using the general configurational parameters described earlier and using a mesh-generating procedure as described next.

Mesh Generator

A mesh generator was developed to replicate the outer surface of the aerobrake configured as a forward spherical shell connected to a conical shell that terminates at an aft cutting plane. This aft cutting plane may be perpendicular to the axis of symmetry for a symmetrical aerobrake, or at an angle β to it in the most general case.

Nodes are generated along the outer surface for a fixed azimuth and along circles for a fixed axial coordinate. Once the outer nodes are generated, a lower set of nodes is also generated inside either at a fixed or variable depth along the normals. Eighteen member space frame elements are generated in each of the hexagonal building blocks (see Fig. 3). The number of elements in both the spherical and conical sections are program parameters and can be chosen by the user. This scheme was chosen for its simplicity and for its ability to develop a number of aerobrake structure configurations easily. Figure 3 presents a typical petal of the aerobrake support structure with two elements in the spherical and two elements in the conical sections. Sixteen of these petals are connected to form the aerobrake structure, as in Fig. 2, that will support the aeroshell shown in Fig. 1. A complete model of a space frame structure consisting of 784 space frame elements with 196 nodes is shown in Fig. 4. This model was developed with two subdivisions in the spherical and three subdivisions in the conical section. A 10-ft constant depth of the space frame structure was used in this model. This construction forms a stable space frame structure. This model was used in all of the studies reported in this paper.

Loading

The loading is assumed to be of constant pressure normal to the aeroshell. On the outer surface of the support structures and on each of the quadrilateral surfaces a thermal protection

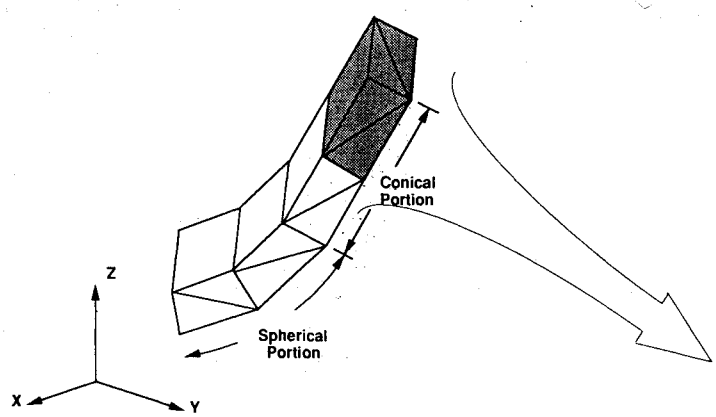

a) Typical Pedal of the aerobrake

	No. of Members
Front face	4
Back Face	4
Front - Back Connections	4
Diagonals	4
Space Diagonals	2
Total	18

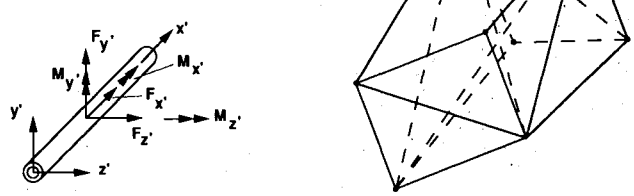

b) Space frame element and hexagonal building block

Fig. 3 Typical petal of the aerobrake and the building block of the space frame structure.

system is assumed to exist. The aerodynamic load is assumed to act normal to this quadrilateral and the loads are transmitted to the four nodes of the quadrilateral as the equivalent loads F_x, F_y, and F_z and three moments M_x, M_y, and M_z at each of the four corners of the quadrilateral panel (see Fig. 5). This is accomplished by equating the work done by the pressure on the quadrilateral panel and the consistent nodal loads $\{F\}$ on the nodal displacements $\{U\}$ as,

$$\frac{1}{2}\int_{\Omega} p(x',y')\cdot w(x',y')\,d\Omega = \frac{1}{2}\{U\}^T\{F\} \tag{1}$$

where $w(x',y')$ is the normal deflection at any point (x',y') on the quadrilateral element, and $p(x',y')$ is the magnitude of the normal pressure at any point (x',y') of the quadrilateral panel element, and

$$\{U\}^T = \{U_i \quad U_j \quad U_k \quad U_l\}$$
$$\{F\}^T = \{F_i \quad F_j \quad F_k \quad F_l\} \tag{2}$$

where

$$\{U_i\} = \{u \quad v \quad w \quad \theta_x \quad \theta_y \quad \theta_z\}_i \tag{3}$$

$$\{F_i\} = \{F_x \quad F_y \quad F_z \quad M_x \quad M_y \quad M_z\}_i \tag{4}$$

and so on. The u_i, v_i, and w_i are the displacements, and θ_{xi}, θ_{yi}, and θ_{zi} are the slopes at the ith node in the global Cartesian coordinate system (see Fig. 5). The integrations involved in Eq. (1) are carried out by mapping[7] the quadrilateral to a parent element in the (ξ, η) plane with $-1 \le \xi \le 1$ and $-1 \le \eta \le 1$. The normal deflection is assumed to be the deflection interpolation functions for a quadrilateral element in parent coordinates (ξ, η)

$$w(\xi,\eta) = a_1 + a_2\xi + a_3\eta + a_4\xi^2 + a_5\xi\eta + a_6\eta^2 + a_7\xi^3 + a_8\xi^2\eta + a_9\xi\eta^2 + a_{10}\eta^3 + a_{11}\xi^3\eta + a_{12}\xi\eta^3 \tag{5}$$

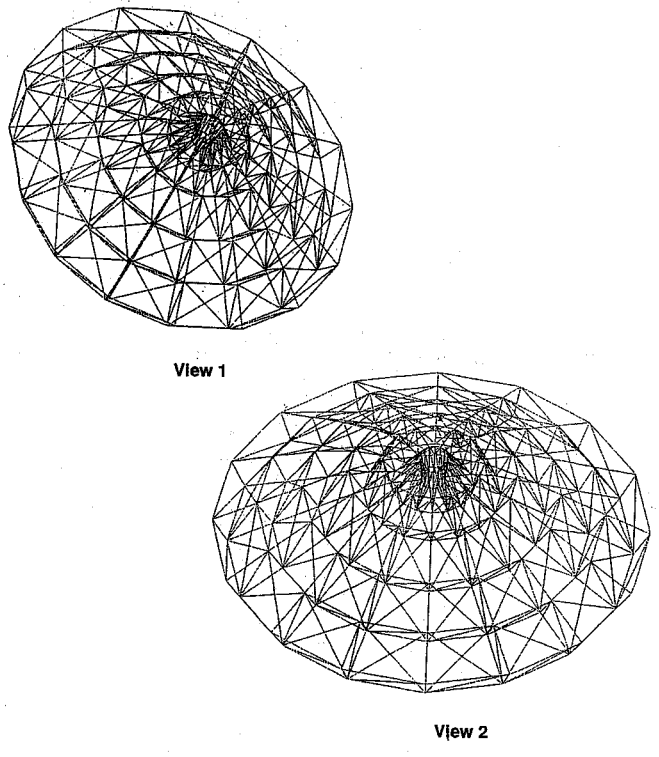

Fig. 4 Aerobrake space frame structure.

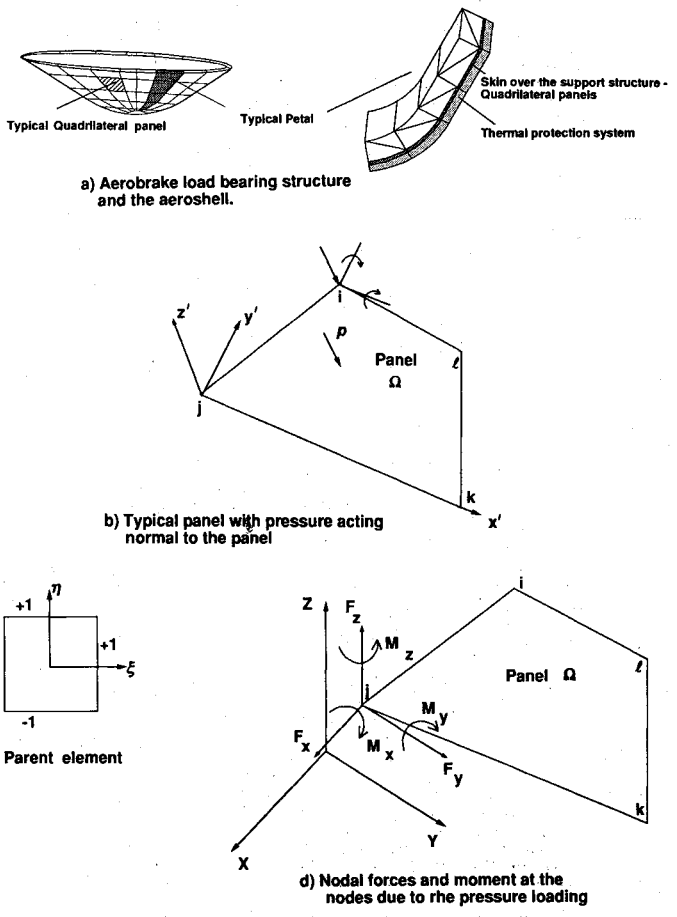

Fig. 5 Aerodynamic loading on the aeroshell and loading at the nodes.

This procedure is repeated for all of the quadrilateral panels, and the resulting consisting loads are assembled into a global load vector as is customary in finite element analysis.[7]

Analysis and Sizing Algorithm

Analysis

The aerobrake load-bearing structure is analyzed by a finite element program with space frame elements. The loads due to the aerodynamic pressures are calculated as equivalent nodal forces and moments as already described.

Two major types of support conditions were used. In the first type, all of the nodes on the circumference of the base of the aerobrake (with 135-ft diameter) are assumed to be rigidly connected to a rigid base to which the payload is attached. Therefore all displacements and rotations at all of the 16 nodes on this circumference were prescribed zero values. In the second type of support conditions only 8, every other node, of the 16 nodes were restrained in the aforementioned manner. Next the supports were relocated at nodes that are closer to the vertex of the aerobrake. Figures 6b and 6c show the support locations, on a typical petal, at the base and at the cone-sphere junction. The effect of the support location on the aerobrake deformations and the aerobrake mass are discussed later.

The aerobrake structure shown in Fig. 2 has 16 petals and 16 planes. Thus the structure with $\beta = 0$, constant pressure loading, and type-1 support conditions exhibits cyclic symmetry. Thus one can use only one petal and analyze this aerobrake configuration. However, this symmetry was not exploited because development of a general analysis program is the main goal of this work. The finite element analysis showed, however, the cyclic symmetries present in the problem configuration.

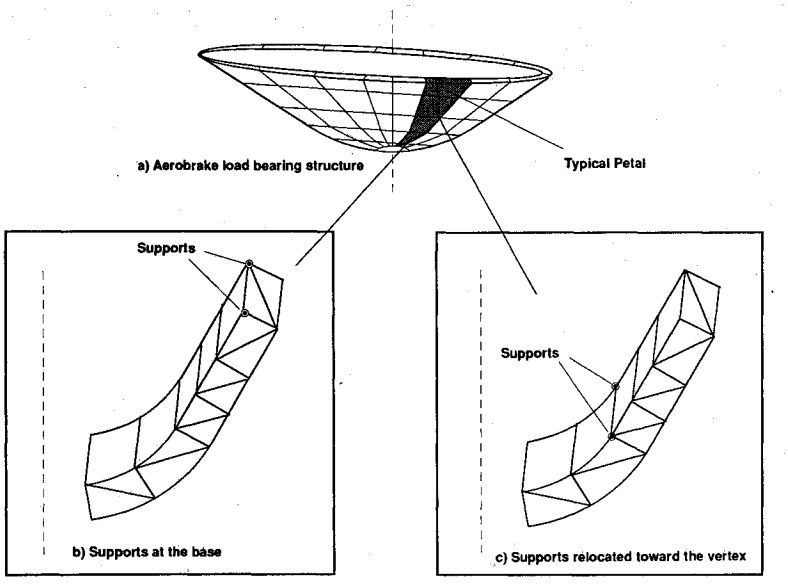

Fig. 6 Various support locations on the aerobrake structure.

Sizing Algorithm

The FE analysis and the sizing algorithm are built into a single complete computer program. Figure 7 presents the flow chart of this combined analysis program. First, all of the space frame members were assumed to be tubular members with the same cross-sectional dimensions, outer radius R_o, and thickness t. A suitable material for the members is chosen with Young's modulus E, and stress allowables Σ_T and Σ_C in tension and compression, respectively. The moments of inertia of the members about the y' and z' axes are equal to (see Fig. 3b)

$$I_{y'y'} = I_{z'z'} = (\pi/4) \cdot [R_o^4 - (R_o - t)^4] \tag{6}$$

The cross-sectional areas of the members are

$$A = \pi[R_o^2 - (R_o - t)^2] \tag{7}$$

The analysis starts with assuming that all the members in the structure have the same cross section and size, R_o and t. The finite element analysis is performed, and the deformations and stress in each of the members are calculated. The stresses are compared with the allowables and a new thickness is calculated for each member. With the new thicknesses, the new aerobrake mass is evaluated. If the new mass W_{j+1} is different from the old mass W_j by less than 2% then the algorithm is terminated. On the other hand, if W_{j+1} is different from W_j by more than 2%, the finite element analysis is continued with the new areas of cross section and moments of inertia to calculate the new displacements and stresses. This iterative procedure is continued until the mass condition

$$\left|\frac{W_{j+1} - W_j}{W_j}\right| \leq 0.02 \tag{8}$$

is satisfied.

The most important step of this iterative process is the procedure to calculate the new thickness required for each of the members. This is accomplished by considering the stresses due to 1) simple axial tension or compression, 2) combined axial and bending loading, and 3) Euler buckling; as well as determining the thickness required under each of these conditions, and choosing the largest value of the thicknesses that satisfies all criteria that apply.

At the end of each finite element analysis, the forces $F_{x'}$, $F_{y'}$, and $F_{z'}$ and moments $M_{x'}$, $M_{y'}$, and $M_{z'}$ at either end of the space frame member are known in the local member coordinate (x',y',z') system (see Fig. 3b). These forces and moments are used to calculate the new thickness for each of the preceding conditions.

Simple Axial Tension or Compression

The new thickness is computed from equating the axial stresses in the member to the allowables as

$$\frac{F_{x'}}{A} = \Sigma' \tag{9}$$

where Σ' is either Σ_T or Σ_C depending on whether F_x' is tensile or compressive, respectively, in the member. The new thickness can be calculated from

$$t_n = R_o - R_o\sqrt{1 - F_{x'}/(\pi R_o^2 \Sigma')} \tag{10}$$

If the term under the radical in Eq. (10) becomes negative, then a solid cross-sectional member is needed and the new radius of this member can be calculated as

$$R_{o_n} = \sqrt{F_{x'}/(\pi\Sigma')} \tag{11}$$

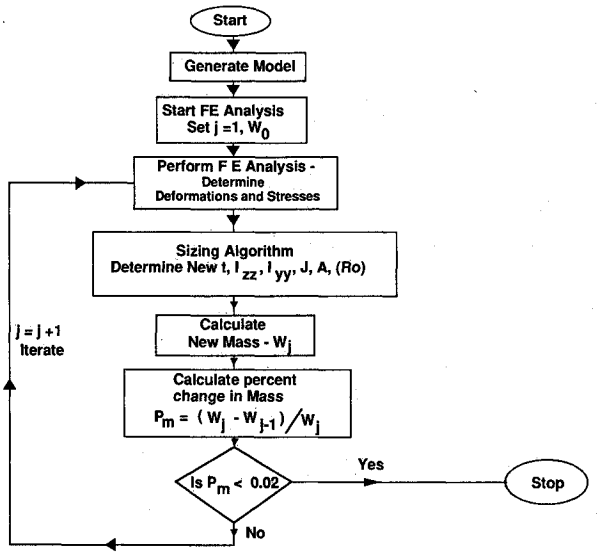

Fig. 7 Flow chart for the analysis and sizing procedure.

Combined Bending and Axial Loading

For the combined loading, the maximum stresses are calculated at either end of the member, and these stresses are compared with the allowable to arrive at the new thickness.

1) Maximum stress at node i of the member: The maximum moment in the cross section at node i (see Fig. 3b) of the member is

$$M_{\max_i} = \sqrt{M_{z_i}^2 + M_{y_i}^2} \tag{12}$$

Thus the maximum stress in the cross section is either σ_1 or σ_2, where

$$\sigma_1 = -\frac{F_{x_i}}{A} + M_{\max_i}\frac{R_o}{I}$$

$$\sigma_2 = -\frac{F_{x_i}}{A} - M_{\max_i}\frac{R_o}{I} \tag{13}$$

2) Maximum stress at node j of the member: The maximum moment in the cross section at node j (see Fig. 3b) of the member is

$$M_{\max_j} = \sqrt{M_{z_j}^2 + M_{y_j}^2} \tag{14}$$

where

$$M_{z_j} = M_{z_i} - F_{y_i} \cdot l$$

$$M_{y_j} = M_{y_i} + F_{z_i} \cdot l \tag{15}$$

In Eq. (15), l is the length of the space frame member. Using these moments, the maximum stress in the cross section at node j is either σ_3 or σ_4, where

$$\sigma_3 = -\frac{F_{x_i}}{A} + M_{\max_j}\frac{R_o}{I}$$

$$\sigma_4 = -\frac{F_{x_i}}{A} - M_{\max_j}\frac{R_o}{I} \tag{16}$$

From the four stresses σ_1, σ_2, σ_3, and σ_4 in Eqs. (13) and (16), maximum tension and compressive stresses σ_T and σ_C can be determined. These stresses are used to calculate the new thickness, t_T for tension and t_C for compression, as

$$t_T = R_o - \sqrt{R_o^2 - A(\sigma_T/\Sigma_T)}$$

$$t_C = R_o - \sqrt{R_o^2 - A[(-\sigma_C)/(-\Sigma_C)]} \tag{17}$$

If the term in the radical in Eq. (17) is less than zero, then a solid cross-sectional member is required and the new radius R_{o_n} of this member can be calculated from either of the following equations:

$$R_{o_n} = \sqrt{\frac{A\sigma_T}{\Sigma_T}}$$

$$R_{o_n} = \sqrt{\frac{A(-\sigma_C)}{(-\Sigma_C)}} \tag{18}$$

Euler Buckling

Assuming the space frame members that are in compression act as pin-ended columns, the new thicknesses of the members are computed by considering Euler buckling. Obviously, this assumption is in contradiction with the assumption of space frame structure (with rigid joints). However, this assumption can be viewed as a severe restriction and hence will lead to very conservative aerobrake mass estimates. The present mass obtained with conservative assumptions like pin joints needs to be compared with the mass due to propulsion braking to check if the present mass is competitive.

The new thickness based on pin-ended column buckling is obtained by first calculating the new moment of inertia required as

$$I_N = \frac{F_{x'} l^2}{\pi^2 E} \tag{19}$$

and the new thickness from

$$t_E = R_o - \left(R_o^4 - \frac{4I_N}{\pi}\right)^{1/4} \tag{20}$$

If the term in the parentheses in Eq. (20) is less than zero, then a solid cross-sectional member is required to withstand the compressive loads. The new radius of the solid cross section can be calculated from

$$R_{o_n} = \left(\frac{4I_N}{\pi}\right)^{1/4} \tag{21}$$

The largest of the thicknesses obtained from Eqs. (10), (17), and (20) is chosen as the new thickness of the space frame member. If any of the criteria require a solid section, then the new radius of the member is taken from the largest of the values in Eqs. (11), (18), or (21).

On the other hand, in lightly loaded regions the algorithm may require very small thickness members. However, very thin tubular sections may not be practical, and so if the maximum thickness required by the algorithm is smaller than the minimum thickness $t_{\min}$ stock, then $t_{\min}$ is used as the thickness for such members.

With these new thicknesses (and new radii, if solid sections are needed), the FE analysis is repeated until the aerobrake mass converges as indicated in the flow chart in Fig. 7.

Results and Discussion

The aerobrake support structure shown in Fig. 4 is analyzed and sized for minimum mass. In these analyses and sizing the following quantities are assumed. The space frame members are assumed to have a tubular cross section with 3-in. outer radius and are assumed to be initially 0.5 in. thick. Constant aerodynamic loading of 2 psi normal pressure to the aeroshell is assumed corresponding to a 6-g deceleration. A factor of safety of 1.4 is used and the loads on the aerobrake are scaled up by this factor in the analysis. Thus a normal pressure of 2.8 psi is used in the analysis. This pressure distribution results in a total load of about 5.60×10^6 lbf for the 135-ft aerobrake. The spacecraft mass can be calculated as follows:

Spacecraft mass = total load without the factor of safety/deceleration
= 3,998,694/6
= 666,449 lbm

The analyses and sizing are performed for two commonly used material systems for aeroshell structures. These are a 7075-T6 lightweight Al-alloy material and a high modulus graphite/epoxy material. The material properties and other pertinent quantities used in the analyses are presented in Table 1 and were chosen to match those used by Dorsey and Mikulus[2,3] and Washington and Klang.[5,6]

A $[\pm 10 \text{ deg}]_{ns}$ stacking sequence was used for the graphite/epoxy composite material struts by Dorsey and Mikulus because for a $[\pm\theta]_{ns}$ stacking sequence strut the minimum mass design occurs when the local and Euler buckling stresses become equal and this occurs when $\theta = 10$ deg (see Refs. 2 and 3).

Composite Material Struts

Figure 8 presents the convergence of the aerobrake mass as a function of the sizing algorithm's iterations. Here the consistent loads are computed on the quadrilateral panels and were

Table 1 Material properties of Al-alloy and graphite/epoxy composite and other quantities used in the analyses

Property	Al-alloy	Graphite/epoxy composite[a]
Young's modulus, E, psi	10×10^6	39.795×10^6
Shear modulus, G, psi	3.846×10^6	2.061×10^6
Density, ρ, lb/in.^{3}	0.101	0.063
Σ_T, ksi	82	100
Σ_C, ksi	80	100
R_o, in.	3.0	3.0
t, in.	0.5	0.5
t_{min}, in.	0.006	0.006

[a][± 10 deg]$_{ns}$ stacking sequence with unidirectional properties, $E_{11} = 44.3 \times 10^6$ psi, $E_{22} = E_{33} = 10^6$ psi, $G_{12} = 0.85 \times 10^6$ psi, $\nu_{12} = 0.3$.

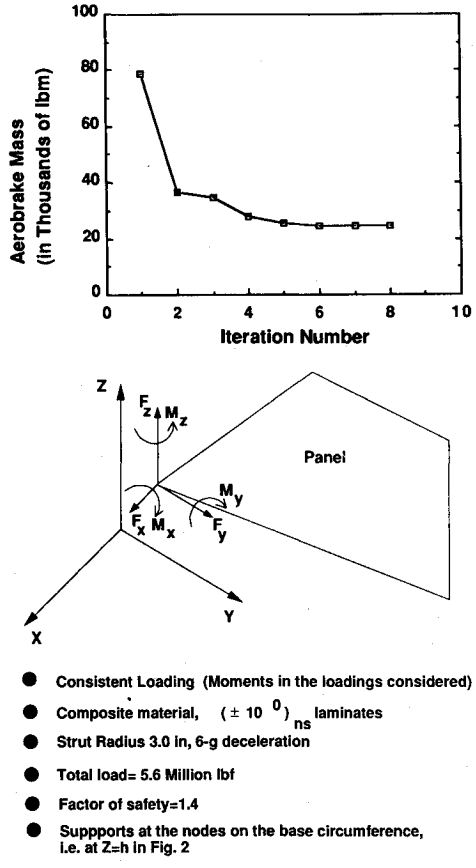

Fig. 8 Convergence of the sizing algorithm for composite material struts and 6-g deceleration—consistent loading.

assigned at the joints. Initially the aerobrake mass starts very high (about 80,000 lbm, corresponding to a 3-in. radius and 0.5-in. thick strut). After the first iteration the weight drops by a factor 2 to about 40,000, and in about 6 to 8 iterations the aerobrake mass stabilizes to about 29,000 lbm. The convergence of the aerobrake mass is rapid and monotonic.

Figure 9 presents similar results for the same configuration but with lumped loading. The lumped loading without moments closely represents the loading if a space truss structure is used. An analysis of the space frame structure without the moments in the loading probably resembles the actual case because neither of the other two cases (space frame with rigid joints or space truss with pin joints) are completely realistic. Figure 9 shows monotonic convergence and the minimum aerobrake mass of 10,990 lbm.

Al-Alloy Struts

Figure 10 presents similar results for Al-alloy material struts. The convergence to the minimum aerobrake mass is very similar to that with composite material struts. However, comparison of Figs. 8–10 shows that the Al-alloy struts are considerably heavier than the composite material struts.

Comparison with Other Results

Dorsey and Mikulus[2,3] analyzed a 120-ft aerobrake of lightweight erectable tetrahedral support truss structure. Composite material struts with [± 10 deg]$_{ns}$ stacking sequence laminates were used. A tetrahedral truss with a three-strut design and six support points and six ring configuration for various decelerations from 2 to 6 g were analyzed. For a 6-g deceleration (with 2 psi pressure on the aerobrake), the tetrahedral truss total mass was obtained as 17,000 lbm (see Fig. 24 of Ref. 2). This value is the total mass of the aerobrake and is based on the assumption that the mass of the joints is equal to the mass of the struts. The spacecraft mass assumed in Ref. 2 was 450,000 lbm. Thus the mass of the tetrahedral truss aerobrake is about 3.8% of the spacecraft mass.

The mass computed in Fig. 9 for a 135-ft aerobrake with the same composite material struts and lumped loading is 10,990 lbm. This is the mass obtained when all of the nodes on the circumference at the base of the aerobrake are fixed. Note also that this is the mass for the struts alone. Using the assumption that the mass of the joints is equal to that of the strut mass, that total mass of the present space frame aerobrake structure will be equal to 10,990 + 10,990 = 21,980 lbm. Thus the mass of the space frame aerobrake structure is 3.3% (21980/666,449 = 0.033) of the spacecraft mass. This mass ratio agrees well with the mass for a tetrahedral truss aerobrake.

In making the comparison, the present results with the lumped loading are considered because the loading on the tetrahedral truss structure is applied in a similar manner as the lumped loading. On the other hand, if one uses the results in Fig. 8, for consistent loading (the loading that includes moments) the present space frame aerobrake structure will be heavier by about a factor 2. For this case the mass of the aerobrake structure is about 8.7% of the spacecraft mass.

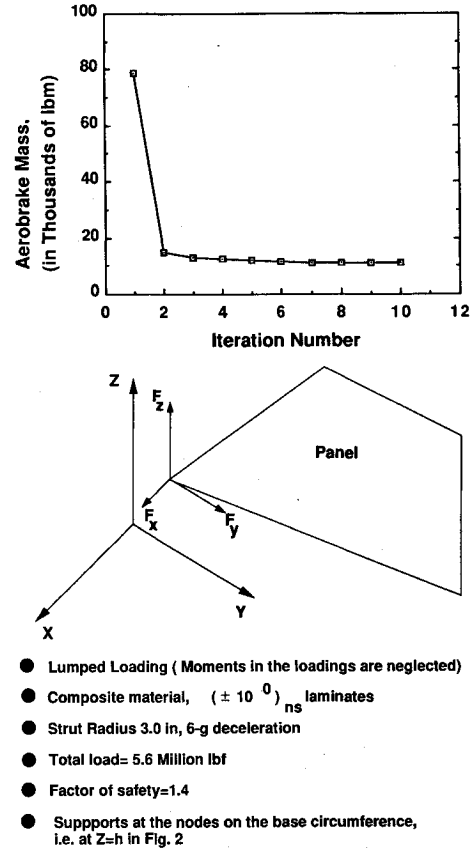

Fig. 9 Convergence of the sizing algorithm for composite material struts and 6-g deceleration—lumped loading.

Thus the mass ratios obtained with the space frame structure are in good agreement with those obtained with the tetrahedral truss aerobrake structure.

Types of Support Conditions

Two major types of support conditions were used. In the first type, all of the nodes on the circumference at the base of the aerobrake (with 135-ft diameter) are assumed to be rigidly connected to a rigid base. Therefore all displacements and rotations at the 16 nodes on this circumference were prescribed zero values. In the second type only 8 nodes, that is, every other node of the 16 nodes, were restrained in the aforementioned manner. The differences in the minimum mass of the aerobrake between the two support conditions were negligible. Thus the first type of support that prescribes zero displacements and rotations at all of the 16 nodes was used in the rest of this study.

Effect of Support Location on the Aerobrake Mass

To study the effect of support location on aerobrake mass, as shown in Fig. 6, the 16 support points are moved to new nodes progressively closer to the vertex of the aerobrake. Figure 11 shows minimum aerobrake mass computed by the sizing algorithm as a function of the diameter of the circle on which the support nodes lie, the support nodal circle. As the support points move closer to the vertex, the aerobrake mass increases and the minimum mass was obtained when the supports are near but not at the base of the aerobrake and are on a circle with a diameter of about 75% of the base diameter.

In this figure, the space frame aerobrake structure results are also compared with those of a doubly curved truss aerobrake structure[5,6] with the same composite material struts, pressure distribution, factor of safety, etc., as those used in this paper. The results of the aerobrake strut mass given in Fig. 6 of Ref. 6 for a 120-ft aerobrake are plotted in Fig. 11 along with the present results for a 135-ft aerobrake. The respective spacecraft masses were 450,000 lbm for the truss aerobrake and 666,649 lbm for the present space frame aerobrake. The minimum strut mass of the space frame aerobrake structure was obtained as about 9400 lbm (or about 1.4% of the spacecraft mass) and occurred where $(d/d_{max}) = 0.75$, whereas the truss aerobrake structure minimum mass was 7000 lbm (or about 1.6% of the spacecraft mass) and occurred when $(d/d_{max}) = 0.80$. Thus the location of the minimum mass and the minimum mass ratio with the present analysis agree well with those obtained in Ref. 6.

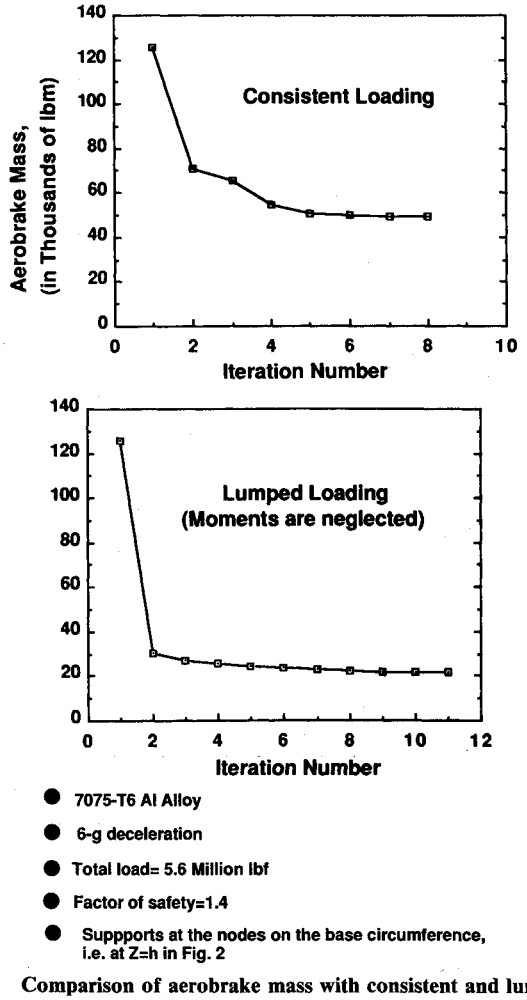

Fig. 10 Comparison of aerobrake mass with consistent and lumped loading for Al-alloy struts.

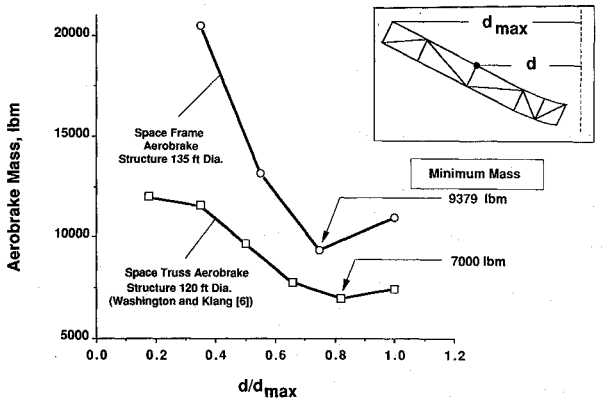

Fig. 11 Effect of support location on aerobrake total mass (composite material struts).

Further Studies

The objectives of this work are to develop an analysis and sizing algorithm of a typical Mars mission aerobrake. After these objectives are reached, several additional analyses can then be performed:

1) Parametric studies involving the number of nodes, number of "bays" in the conical and spherical portions, depth of each bay, number of petals, angle of the oblique cutting plane β, etc., can be performed to arrive at the optimal aerobrake structural configuration.

2) In the sizing algorithm, in addition to the criteria used in this paper, stresses due to torsion, torsion buckling, and combined bending and torsion can be considered to determine new thicknesses of the struts. These additional criteria present no additional difficulties but only make the sizing algorithm more complicated.

3) Additional analyses such as vibration, flutter, overall buckling, stiffness requirements, buckling of parts of the structure (such as one, two, or more of the petals), etc., can be performed.

Concluding Remarks

Aerobrake structures that can be used in entry into Martian atmosphere are studied. A cone-sphere aerobrake configuration is considered in this study. Using this aerobrake configuration, a space frame load-bearing structure is proposed. A mesh generator that develops a complete finite element model of a space frame structure with few configurational parameters was developed. With this mesh generator a variety of cone-sphere aerobrake space frame load-bearing structures can be developed very easily.

A finite element analysis program that analyzes space frame aerobrake structures was developed. A sizing algorithm that arrives at the minimum mass space frame aerobrake structure was also developed. This algorithm is integrated into the finite element analysis program so that the analysis and sizing are performed in one single run. A typical aerobrake configuration with 135-ft diameter was analyzed and sized. The minimum mass of the aerobrake structure necessary to withstand a 2 psi constant aerodynamic pressure (with a factor of safety of

1.4) was calculated with the sizing algorithm for two types of loading assumptions. In the first case, the loading is assumed to be such that the aerodynamic pressure acts on quadrilateral panel (heat shield) elements and is transmitted to the joints of the space frame structure as concentrated loads. This assumption is termed as the lumped loading. In the second case, the loading on the quadrilateral panels is assumed to be transmitted as concentrated joint loads and moments. This assumption is termed as the consistent loading. The minimum mass for the lumped loading is only about 3.3% of the spacecraft mass. On the other hand, when the consistent loading is used, the minimum mass is about 8.7% of the spacecraft mass. These values correspond to the case when high strength and lightweight composite materials are used for the space frame struts. The masses are heavier if aluminum alloy is used as the strut material. In the literature, minimum mass aerobrake structural configurations were reported with a lightweight erectable aerobrake structure and a doubly curved (part spherical) aerobrake truss structure using composite materials. The mass of the optimized aerobrake structure by the present analysis and the sizing algorithm are in good agreement with the mass obtained with the other aerobrake configurations from the literature.

The effect of support location on the aerobrake mass was also studied by relocating the support nodal circles toward the vertex of the aerobrake. As the support points move closer to the vertex, the aerobrake mass first reduces and then shows an increase. The minimum mass was obtained when the supports are near but not at the base of the aerobrake and are on a circle with a diameter of about 75% of the base diameter.

The finite element program and the sizing algorithm developed in this paper should be useful to analyze and size other space frame aerobrake structural configurations.

Acknowledgments

This work was supported under NASA Headquarters Grant NAGW-1331 to the Mars Mission Research Center at North Carolina State and North Carolina A&T State Universities. This work was performed at the North Carolina A&T State University when the first author was a research professor there. The authors are grateful to J. H. Starnes Jr. of the NASA Langley Research Center for many discussions and suggestions. The computations presented in this work were carried out on a Cray Y-MP at the North Carolina Supercomputing Center, Research Triangle Park, North Carolina. The authors take this opportunity to express their gratitude to all of these organizations. Finally, the authors are grateful to the reviewers of this paper for many valuable suggestions and comments.

References

[1]Walberg, G. D., "A Review of Aerobraking for Mars Missions," International Astronautical Federation, IAF Paper 88-196, Oct. 1988.

[2]Dorsey, J. T., and Mikulus, M. M., Jr., "Preliminary Design of a Large Tetrahedral Truss/Hexagonal Heatshield Panel Aerobrake," NASA TM 101612, Sept. 1989.

[3]Dorsey, J. T., and Mikulus, M. M., Jr., "Preliminary Design of a Large Tetrahedral Truss/Hexagonal Heatshield Panel Aerobrake," AIAA Paper 90-1050, April 1990.

[4]Walberg, G. D., " A Survey of Aeroassisted Orbit Transfer," *Journal of Spacecraft and Rockets,* Vol. 22, No. 1, 1985, pp. 3–18.

[5]Klang, E. C., and Washington, G. N., "Aerobrake Construction Concepts for the Mars Mission," *Proceedings of the Space '90 Conference,* American Society of Mechanical Engineers, Vol. 1, Albuquerque, NM, April 1990.

[6]Washington, G. N., and Klang, E. C., "Modeling and Analysis of Doubly Curved Aerobrake Truss Structures," *Proceedings of the Space '92 Conference,* American Society of Mechanical Engineers, Denver, CO, May 1992.

[7]Zienkiewicz, O. C., *The Finite Element Method,* 3rd ed., McGraw-Hill, New York, 1987.

Earl A. Thornton
Associate Editor